Heterogeneous & Homogeneous & Bio- & Nano-

CHEMCATCHEM

CATALYSIS

Accepted Article

Title: Effect of vapor-phase-treatment to CuZnZr catalyst on the reaction behaviors in CO2 hydrogenation into methanol

Authors: Shuyao Chen, Junfeng Zhang, Peng Wang, Xiaoxing Wang, Faen Song, Yunxing Bai, Meng Zhang, Yingquan Wu, Hongjuan Xie, and Yisheng Tan

To be cited as: *ChemCatChem* 10.1002/cctc.201801988

Link to VoR: http://dx.doi.org/10.1002/cctc.201801988

A Journal of

ChemPubSoc Europe

WILEY-VCH

www.chemcatchem.org

Effect of vapor-phase-treatment to CuZnZr catalyst on the reaction behaviors in CO_2 hydrogenation into methanol

Shuyao Chen,[a,b] Junfeng Zhang,*[a] Peng Wang,[a,b] Xiaoxing Wang,[a] Faen Song,[a] Yunxing Bai,[a,b] Meng Zhang,[a,b] Yingquan Wu,[a] Hongjuan Xie,[a] and Yisheng Tan*[a,c]

Abstract: CuZnZr catalysts prepared by co-precipitation method were treated by vapor-phase-treatment (VPT) method, and used for the synthesis of methanol for CO_2 hydrogenation. Compared with conventional co-precipitation method, this VPT with TPABr induces obvious increases in the particles size of CuO, ZnO and ZrO_2, promotes the formation of the rod-like structure, Zn and Zr enrichments on surface and the presence of more concentration of oxygen vacancies. Due to the increases of particle size especially for CuO particles, the activity of the catalyst for CO_2 hydrogenation to CO (RWGS reaction) is furthest suppressed, leading to dramatical decrease in conversion of CO_2. However, methanol productivity is affected relatively modestly due to the enrichments of Zn and Zr as another active species on the catalyst surface. In addition, catalyst properties and methanol selectivity can be regulated through adjusting the processing time. The catalyst with the processing time of 3 day (CuZnZr-TPABr-3d) catalyst shows a methanol selectivity above 90% and no obvious deactivation appeared in a period of 100 h reaction.

Introduction

Global warming caused by the increase of greenhouse gases emissions and the depletion of fossil fuel due to the growth of economy and population are becoming worldwide challenges to modern society. Among these green-house gases, CO_2 is the most emitted and mainly responsible by so far. Although the efforts to new technologies based on CO_2 storage after capture,[1] the transformation of CO_2 into valuable chemicals and energy carriers, such as methanol and dimethyl ether, appears more interesting and investigable.[2,3] Catalytic hydrogenation of CO_2 to methanol, which is itself an excellent energy carrier and can be transformed to other high value-added chemicals, is a promising pathway that may offer a solution to the green-house gas accumulation and fossil fuel alternatives.[4,5] Unfortunately, the CO_2, this stable molecule, possesses highly thermodynamic stability and low reactivity, leading to low CO_2 conversion in synthesis of methanol.[6] Another barrier is the formation of undesired byproducts CO from the reverse water-gas shift (RWGS) reaction.[7,8] Therefore, the development and optimization of the efficient catalyst have been a key research to improve the catalyst activity and methanol selectivity.

It is well known that Cu/ZnO-based catalysts ($Cu/ZnO/Al_2O_3$ or $Cu/ZnO/ZrO_2$) prepared by co-precipitation method are employed predominantly in low-temperature methanol synthesis process.[4,9,10] The Cu/ZnO interface has been reported as an unique adsorption site of CO_2[11] and zirconia can act as a promising support and promoter enhance the copper dispersion as well as the surface basicity.[12,13] Due to these advantageous properties of ZrO_2, $Cu/ZnO/ZrO_2$ catalysts are more effective for methanol synthesis in CO_2 hydrogenation reaction.[14,15,16] However, one of the problems for applying these catalysts in CO_2 hydrogenation is that methanol selectivity is still not so high as expected due to the presence of competitive reverse water-gas shift (RWGS) reaction. Hereof, with the aim of improving the methanol selectivity, various modified methods, such as tuning catalyst composition,[15,17] ameliorating the methods of preparation[18-22] and pretreatment[23] were generally adopted to obtain distinctive properties, and some important progresses have been made.[24] Gao et al. [17] synthesized Cu/Zn/Al/Zr hydrotalcite-like precursors with Zr^{4+}: (Al^{3+}+Zr^{4+}) from 0 to 0.7. They found that the CO_2 conversion is related to the surface area and the dispersion of Cu, while the CH_3OH selectivity is connected with the distribution of basic sites on the catalyst surface. Li et al.[25] introduced Ga^{3+} into Cu/ZnO catalyst precursor and found that the presence of small amount of Ga^{3+} can facilitate ZnO support to Zn atoms. They considered that CO_2 conversion and CH_3OH selectivity can be significantly enhanced by increasing the Zn^0 content in their catalytic system. Dong et al.[23] prepared $Cu/ZnO/ZrO_2$ catalysts though precipitation-reduction method. Noted that on the as-prepared catalysts the number of basic sites increase, which has a significant advantage in methanol selectivity compared with conventional precipitation method. Ramli et al.[27] introduced ultrasonic spray precipitation (USP) to prepare Cu-Zn-Al-Zr catalyst. The USP technique dictates the formation of finer Cu crystallites with better particle uniformity and single form of oxide species. The USP-prepared catalyst showed the improved methanol selectivity and yield by 2.7 and 27% compared with conventional precipitation (CP) catalyst. They believed that the improved surface basicity of USP catalyst contributes significantly to the catalytic performance. The above clearly indicated that treatments and modification to catalyst surface (elementary composition, surface structure, etc.) are remarkably effective for methanol synthesis from CO_2.

Herein, we introduced a technique named as vapor-phase-treatment (VPT), to modify the surface structure and active sites over CuZnZr catalysts for CO_2 hydrogenation to methanol. Illustration for the preparation procedure of CuZnZr catalysts

[a] *State Key Laboratory of Coal Conversion, Institute of Coal Chemistry, Chinese Academy of Sciences, Taiyuan 030001, China;*
[b] *University of Chinese Academy of Sciences, Beijing 100049, China;*
[c] *China National Engineering Research Center for Coal-Based Synthesis, Institute of Coal Chemistry, Chinese Academy of Sciences, Taiyuan 030001, China;*
* *Correspondence author:*
Tel./Fax: +86-351-4044287.
E-mail: tan@sxicc.ac.cn; zhangjf@sxicc.ac.cn.
Supporting information for this article is given via a link at the end of the document.

using VPT method is shown in Scheme 1. The original CuZnZr catalyst was first prepared by a co-precipitation method (CP), and then treated by treatment reagents (only H_2O, and TPABr aqueous solution). The as-prepared catalysts were characterized by XRD, N_2 physisorption, SEM, TEM, XPS, XRF, TPR and CO_2-TPD techniques. It was found that the catalyst surface elemental composition is altered and the percentage of the adsorbed oxygen is improved after VPT process, especially using TPABr as the treatment reagent. In the meantime, the processing time using TPABr is able to modulate the degree of enrichment of Zn and Zr on catalyst surface, and tune the content of the adsorbed oxygen. These variation in catalysis surface structure and properties enhances the methanol selectivity and restrains the formation of byproducts CO from the competitive reverse water-gas shift (RWGS) reaction. In addition, the catalytic performances of the as-prepared catalysts for methanol synthesis from CO_2 hydrogenation were discussed deeply in relation to the results of physicochemical characterizations.

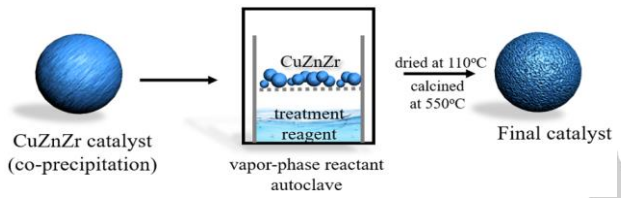

Scheme 1. Illustration for the catalyst preparation by vapor-phase-treatment method.

Results and Discussion

Table 1. Textural and structural properties of the different CuZnZr catalysts.

Catal.	S^a_{BET} (m^2g^{-1})	D^b_{XRD} (nm)		
		CuO	ZnO	ZrO_2
CuZnZr(CP)	76.2	9.80	8.11	-
CuZnZr-H_2O	11.5	21.7	38.4	14.5
CuZnZr-TPABr*	9.13	23.1	41.9	15.2
CuZnZr-TPABr-1d	9.82	21.5	41.2	12.3
CuZnZr-TPABr-3d	7.30	25.0	42.4	14.3
CuZnZr-TPABr-4d	11.6	22.3	47.4	16.8

[a] S_{BET} was calculated by the BET method; [b] Diffraction spectra at 2θ = 38.8 for CuO, 31.8 for ZnO and 30.3 for t-ZrO_2; * CuZnZr-TPABr = CuZnZr-TPABr-2d.

The XRD patterns of the representative catalysts are shown in Fig. 1. The diffraction lines of CuO (JCPDS80-1268) are observed at 2θ of 35.6, 38.8 and 48.9°, and the diffraction lines of ZnO phase (JCPDS36-1451) appear at 2θ of 34.5 and 36.3°.[27] As observed, the diffraction peaks of CuZnZr(CP) are weak, broad (for CuO and ZnO), and even unobvious for ZrO_2. As shown in Fig. 1(a), for the catalysts treated by different treatment reagents, the diffraction peaks become sharp and strong, indicating an increase in the crystallinity and in the particle sizes of CuO, ZnO and ZrO_2. Simultaneously, the processing time also affects the crystallinity (Fig. 1(b)), and the CuZnZr-TPABr-3d sample exhibits the maximum intensity of the diffraction peaks. From Table 1, the calculated sizes of CuO, ZnO and ZrO_2 particles of the catalysts increase noticeably via VPT, and the processing time slightly affects final particle size. The crystallite size of CuO first increases then decreases with the raise of the processing time, and the CuZnZr-TPABr-3d sample exhibits the maximum crystallite size. The BET surface areas derived from N_2 adsorption-desorption are listed in Table 1. It is found that specific surface area for the CuZnZr sample prepared by conventional co-precipitation method is higher than the vapor-phase-treatment samples. Moreover, the surface area first decreases gradually and then raises slightly with the increase of the processing time. The minimum surface area is obtained for CuZnZr-TPABr-3d sample (7.3 m^2 g^{-1}), which might due to its high degree of crystallinity and large particle sizes of metal crystallites.

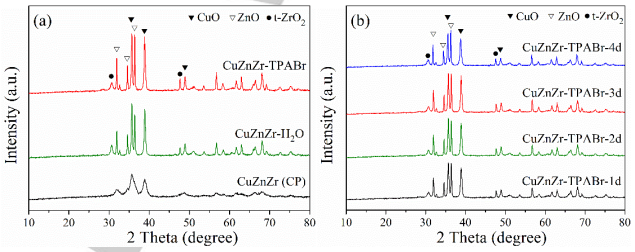

Figure 1. XRD patterns of (a) the CuZnZr(CP) and catalysts treated with different treatment reagents, (b) catalysts treated by TPABr with different processing time.

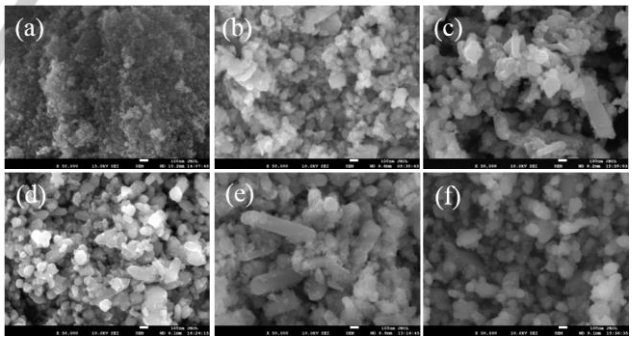

Figure 2. The surface morphology of (a) CuZnZr(CP), (b) CuZnZr-H_2O, (c) CuZnZr-TPABr (= CuZnZr-TPABr-2d), (d) CuZnZr-TPABr-1d, (e) CuZnZr-TPABr-3d, (f) CuZnZr-TPABr-4d.

Fig. 2(a-c) shows the SEM images of the CuZnZr(CP), CuZnZr-H_2O and CuZnZr-TPABr catalysts. The CuZnZr(CP) catalyst consists mainly of aggregated small spherical particles. However, the rod-like particles emerge in the CuZnZr-TPABr catalyst. Moreover, the irregular blocky-shaped particles are found in the samples prepared with different treatment reagents (H_2O, TPABr), whereas, only the CuZnZr-TPABr catalyst possesses the inerratic rod-like particles. The Fig. 2(c-f) depicts

the SEM images of the CuZnZr-TPABr catalysts prepared with different vapor-phase-treatment processing time. It seems that the processing time is able to affect the formed amount of rod-like particles. The rod-like particles appear obviously when the processing time is 2 day, and nevertheless reduce gradually when the processing time is 4 day. The optimum processing time is 3 day which CuZnZr-TPABr-3d catalyst exhibits more rod-like particles than other three catalysts, indicating the processing time plays an important role in forming the rod-like particles. The STEM images of CuZnZr-TPABr-3d catalyst with some rod-like and blocky particles are shown in Fig. 3. It is observed that the Cu and Zr are uniformly distributed on the sample, and nevertheless Zn element is mainly centred on some rod-like particles. This indicates that the main body of rod-like structure is comprised of ZnO, and Cu and Zr are dispersed on ZnO surface. HRTEM images of CuZnZr-TPABr catalyst (Fig. S1) showed four kinds of periodicity of lattice fringe with spacing of 0.234, 0.278, 0.335 and 0.294 nm, ascribed to the (111) plane of CuO, (101) plane of ZnO, (111) plane of ZnO and (011) plane of tetragonal ZrO_2,[23,24] respectively. According to the literature by Li et al.[24] the shinkage of the spacing of (011) plane of ZrO_2 can indicate that solid resolution of ZnZr forms. However, our present CuZnZr-TPABr catalyst shows no any change of the spacing of (011) plane of ZrO_2. Therefore, it is not asserted that the solid metal solution of ZnZr is presented on our present catalyst based on the HRTEM results.

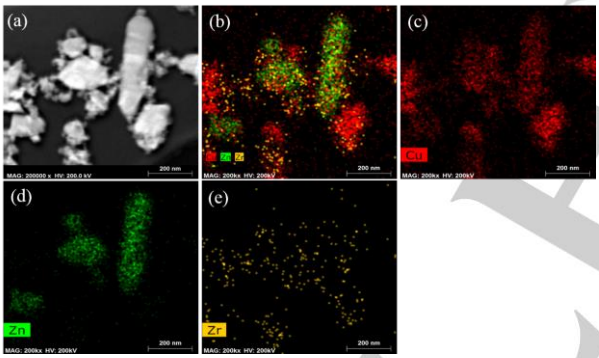

Figure 3. The elemental map of CuZnZr-TPABr-3d catalyst obtained by STEM-EDS. (a) STEM image, (b) STEM-EDS elemental map, (c) Cu channel, (d) Zn channel, (e) Zr channel.

XPS spectra of the CuZnZr(CP) catalyst and catalysts prepared with different vapor-phase-treatment reagents are presented in Fig. S2. The binding energies (BE) of $Cu2p_{3/2}$, $Zn2p_{3/2}$ and $Zr3d_{5/2}$ bands are presented in Table S1, which agree within the error limit with the band position of CuO, ZnO and ZrO_4, respectively.[28,29] As observed, the bands of $Cu2p_{3/2}$ are hardly changable in spite of different preparation condition, that of $Zn2p_{3/2}$ shift to higher binding energies after VPT, and nevertheless only that of $Zr3d_{5/2}$ of CuZnZr-TPABr have an obvious shift to higher binding energies. This indicates that VPT mainly affects the chemical status of Zn species, and usage of TPABr is able to induce change of Zn and Zr BEs at the same time. XPS spectra of the CuZnZr-TPABr catalysts with different processing time are presented in Fig. S3. The datas of the binding energies and compositions are presented in Table 2. With increasing the processing time, the bands of $Zr3d_{5/2}$ shift to higher binding energies slightly. However, when the processing time is 4 days, the bands of $Cu2p_{3/2}$ and $Zn2p_{3/2}$ shift to lower binding energies markedly.

Table 2. Binding energy and atomic concentration (% in molar ratio) data from XPS analysis for different CuZnZr catalysts.

Sample	Cu		Zn		Zr	
	Bulk[a]	Suface	Bulk[a]	Suface	Bulk[a]	Suface
CuZnZr(CP)	32.0	25.9	14.0	18.0	4.02	1.59
CuZnZr-H_2O	31.9	18.0	14.0	18.2	4.11	5.01
CuZnZr-TPABr*	31.9	17.6	14.0	19.2	4.06	7.54
CuZnZr-TPABr-1d	32.0	18.3	13.9	18.5	4.02	6.13
CuZnZr-TPABr-3d	31.9	14.0	14.0	21.0	4.01	7.62
CuZnZr-TPABr-4d	31.6	17.8	14.3	19.5	4.13	8.64

[a] Values in parentheses are concentration normalized to the total atom content measured by XRF; * CuZnZr-TPABr = CuZnZr-TPABr-2d.

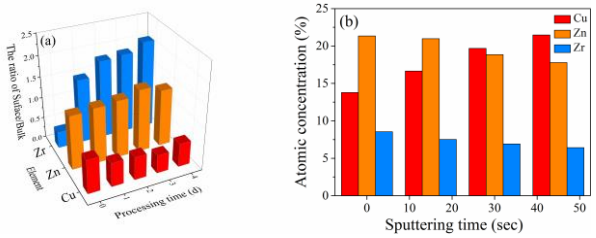

Figure 4. The variation on (a) surface/bulk ratio with the processing time over the catalysts treated by TPABr, (b) atomic concentration of Cu, Zn and Zr versus the sputtering time over CuZnZr-TPABr-3d catalyst.

The compositions of the surface and bulk of the catalysts are summarized in Table 2. The surface compositions of the catalysts were determined by XPS technique and the bulk compositions of the catalyst was estimated by XRF technique. The similar content of Cu, Zn and Zr in bulk compositions is found in different samples. Compared with the CuZnZr(CP) catalyst, vapor-phase-treatment catalysts (CuZnZr-TPABr and CuZnZr-H_2O) show much more considerable depletion of Cu species and the enrichment of Zr. Further noting that the surface of CuZnZr-TPABr catalyst is more enriched in Zn, but the CuZnZr-H_2O catalyst does not show obvious enrichment of Zn on surface. The CuZnZr-TPABr catalyst possesses the characteristic of enrichment of Zn and Zr on catalyst surface simultaneously. The VPT using TPABr affects the bulk compositions hardly, but promotes the enrichment of Zn and Zr on catalyst surface. In addition, as shown in Table 2, the processing time is able to tune the surface element distribution.

The CuZnZr-TPABr-3d sample possesses the maximum surface content of Zn (21.0 at.%), the minimum content of Cu (14.0 at.%) and a proper content of Zr. For the purpose of investigating the various of surface enrichment of metal element with VPT processing time, we introduce the ratio of surface to bulk concentrations (Surface/Bulk) as a standard to evaluate the degree of surface enrichment of metal element. As shown in Fig. 4(a), the degree of enrichment of Zr raises drastically on the surface with the increase of the processing time. The degree of enrichment of Zn first raises then declines, and yet that of Cu exhibits an opposite trend. The CuZnZr-TPABr-3d catalyst possesses the maximum Surface/Bulk ratio of Zn, the minimum Surface/Bulk ratio of Cu and a proper Surface/Bulk ratio of Zr, which is probably attributed to its large quantities of rod-like structure. The depth profiling of elementary composition over CuZnZr-TPABr-3d catalyst was studied by Ar^+ sputtering with using As shown in Fig. 4(b), the atomic concentrations of Zn and Zr decrease gradually, whereas, the atomic concentration of Cu rises observably with increasing the etching time, indicating that Zn and Zr are considerably enriched on the surface and Cu mainly gathered in the bulk, which is in accordance with the STEM results.

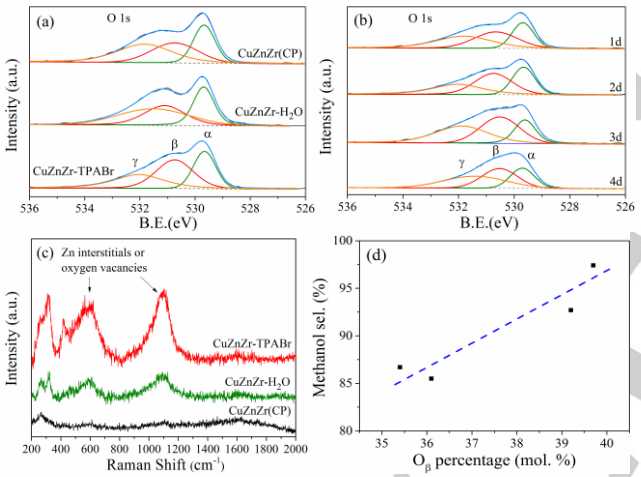

Figure 5. (a) O 1s XPS spectra of the CuZnZr(CP), CuZnZr-H_2O and CuZnZr-TPABr catalysts; (b) O 1s XPS spectra of the catalysts treated by TPABr with different processing time; (c) Raman spectrum of CuZnZr(CP), CuZnZr-H_2O and CuZnZr-TPABr catalysts; (d) the relationship between methanol selectivity and the percentage of O_β peak.

The O1s X-ray photoelectron spectra of the CuZnZr catalysts with different treatment reagents are shown in Fig. 5(a). All samples show three predominant peaks (denoted as α, β, and γ), which are attributed to the lattice oxygen, surface-adsorbed oxygen, and surface hydroxyl species, respectively.[30] The peak of surface-adsorbed oxygen (β peak) is commonly related to the presence of oxygen vacancies on sample surface.[31] The calculation for relative concentration (listed in Table 3) reveals that the CuZnZr-TPABr catalyst possesses more concentration of oxygen vacancies than the CuZnZr(CP) and CuZnZr-H_2O catalysts. With increasing the vapor-phase-treatment processing times, the concentration of β peak first increases until the processing time is 3 days and then decreases, indicating that the processing time of 3 days is the most favourable for increasing the concentration of β peak as shown Fig. 5(b) and Table 3.

Fig. 5(c) shows the Raman spectrum for the catalysts, wherein, the bands at ca. around 600 cm^{-1} and 1100 cm^{-1} are ascribed to the intrinsic oxygen vacancies.[31] Relatively stronger peak intensity of the CuZnZr-TPABr, than that of the other catalysts, indicates the treatment with TPABr effectively promotes the formation of more oxygen vacancies, which is in accordance with the XPS results.

Table 3. Surface oxygen atomic concentration and percentage (% in molar ratio) data from XPS analysis for different CuZnZr catalysts.[a]

Sample	Total surface oxygen concentration (%)	Surface oxygen atomic percentage (% in molar ratio)		
		O_α	O_β	O_γ
CuZnZr	54.5	28.7	31.1	40.2
CuZnZr-H_2O	58.8	38.6	33.5	27.8
CuZnZr-TPABr*	55.7	29.9	39.2	30.9
CuZnZr-TPABr-1d	57.1	27.0	35.4	37.6
CuZnZr-TPABr-3d	57.4	21.7	39.7	38.7
CuZnZr-TPABr-4d	54.1	25.2	36.1	38.8

[a] O_α, O_β and O_γ are attributed to lattic oxygen Olatt (O^{2-}), surface absorbed oxygen Oads (O^-, O_2^- or O_2^{2-}) and oxygen-containing groups, respectively; * CuZnZr-TPABr = CuZnZr-TPABr-2d.

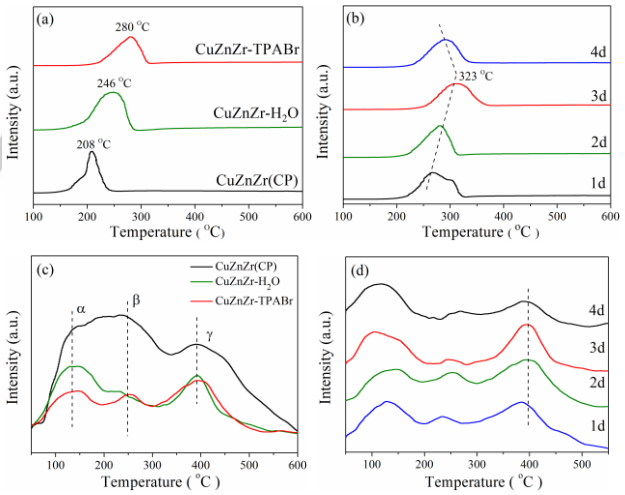

Figure 6. H_2-TPR profiles of (a) CuZnZr(CP), CuZnZr-H_2O and CuZnZr-TPABr catalysts, (b) catalysts treated by TPABr with different processing time; CO_2-TPD profiles of (c) CuZnZr(CP), CuZnZr-H_2O and CuZnZr-TPABr catalysts, (d) catalysts treated by TPABr with different processing time.

In order to investigate the reduction behaviors of the catalysts, the TPR measurements of the prepared catalysts were carried out. As shown in Fig. 6(a and b), the reduction profiles of all the samples exhibit single broad band of H_2

consumption in the range of 200-330 °C, which is related to the reduction of CuO phase,[32] Since ZnO and ZrO_2 are not reduced within the experimental regions. From Fig. 6(a), the reduction peak of CuO shifts towards high temperature with the process of VPT. This VPT process might enhance the interaction between Cu^{2+} and metal oxides of Zn and Zr, resulting in hard reducibility of the Cu^{2+} species, especially for treatment with TPABr. Furthermore, with increasing vapor-phase-treatment processing time, the reduction peaks shifted to higher temperature observed for CuZnZr-TPABr-1d ~ 3d samples and then shifted to lower temperature appearing in CuZnZr-TPABr-4d sample, as shown in Fig. 6(b), revealing that the metallic interaction rises first and then decreases with increasing the vapor-phase-treatment processing time. The CuZnZr-TPABr-3d sample possesses the highest reduction temperature. From the SEM images (Fig. 2), the CuZnZr-TPABr-3d sample possesses larger quantities of the rod-like particles. It suggests that the inerratic rod-like structure appearing in CuZnZr-TPABr-3d sample exhibits a much stronger synergistic effect among multi metallic species and promotes the interaction with metal oxide species. Moreover, the amount of rod-like particles seem to be proportional to the strength of the interaction with metal oxide species so that changing the reduction capacity of Cu^{2+} species. Furthermore, the crystalline size of CuO accurately influences the reduction temperature of catalysts in some degree. From the XRD results (Fig.1), the calculated sizes of CuO, ZnO and ZrO_2 particles of the catalysts increase noticeably via VPT process, as shown in Table 1. The increase in size of CuO particles impedes the reducibility of VPT catalysts, resulting in the higher reduction temperature. Therefore, the variation of reduction temperature of the present catalysts should be co-determined by the changes of particle size and interactions with metals.

The surface base properties of catalysts were investigated by CO_2-TPD technique and desorption profiles of the representative catalysts are presented in Fig. 6(c and d). Generally, the CO_2 desorption profiles can be divided into three Gaussian peaks (denote as α, β, and γ), which correspond to weak, moderate and strong base sites according to the strength of base site, respectively.[23,33] The weak basic sites are originated from the surface hydroxyl group; the medium basic sites are ascribed to the metal–oxygen pairs, such as Zn-O, Zr-O pairs in this case; the strong basic sites are associated with the low-coordination oxygen anions.[23] As shown in Fig. 6(c), the total area of profile on CuZnZr(CP) catalyst is much larger than that of CuZnZr-H_2O and CuZnZr-TPABr catalysts. Further noting that most of the decreases in the peak area are central on the peaks ascribed to α and β, and but γ peak only shows slight decrease, implying VPT has slightly affected the strong basic sites. In comparison of CuZnZr-H_2O and CuZnZr-TPABr, the area of the peaks ascribed to strong basic sites is similar to each other, despite that total area of the former is larger than that of the latter. From the Fig. 6(d), one can also observe that processing time affects the basic properties of catalyst surface certainly, and the process improves the strength of binding of CO_2 adsorbed on the strong basic sites. Generally, the strong basic sites on catalyst surface have been reported to be obviously promotional for CO_2 hydrogenation into methanol.[23] It is known that zirconia possesses surface Lewis basic sites to adsorb CO_2 and it is expected that the alkaline ZnO enhances the affinity of the system to CO_2.[12,34] Based on the above characterizations, it is thought that CO_2 adsorption is significantly affected by the changes on catalyst structure and elemental composition containing Zn and Zr enrichment and oxygen species distribution, which were induced by VPT process.

Shown in Table 4 is catalytic performance in hydrogenation of CO_2 to methanol over CuZnZr catalysts prepared using CP and VPT method. For CuZnZr(CP) catalyst, two main products: methanol and CO are formed, and methanol selectivity is around 55.2%. In the case of the catalysts treated using different regents through VPT method, the activities of hydrogenation of CO_2 on them are obviously different. Compared with CuZnZr(CP) catalyst, the CuZnZr-H_2O catalyst shows slight improvement of methanol selectivity (65.3%). However, it is quite interesting that methanol selectivity of 92.7% is formed on the CuZnZr-TPABr catalyst at 250 °C and 5.0 MPa with 3,000 ml/(g · h) and H_2/CO_2 = 3:1. It is plausible that VPT with TPABr is effective for improving methanol selectivity, whereas the CO_2 conversion decreases via VPT. So, it is easily doubted whether the improved selectivity of methanol is at the expense of the decrease in CO_2 conversion. In order to verify it, the high space velocity of feed gas was used for the present reaction on the untreated catalyst CuZnZr(CP) catalyst based on the consideration in controlling lower CO_2 conversion about 11%, which is near to that on the CuZnZr-TPABr catalyst. As shown in Table 4, increasing the space velocity only induced relatively a slow increase in methanol selectivity, accompanied by the decreased CO_2 conversion. With the space velocity of 55000 ml/(g·h), the CO_2 conversion, finally, decreases to 11.3% which is very approximate to that of CuZnZr-TPABr(11.4%) catalyst, and nevertheless the methanol selectivity(~60.5%) is far lower than that of CuZnZr-TPABr(~92.7%) catalyst. This indicates that the VPT method is able to improve the methanol selectivity because of the modification of the catalyst surface properties. Nevertheless, it should be confessed that the catalyst activity is somewhat passivated via the VPT process, based on the decreased conversion of CO_2, probably ascribled to dramatical increase in the particle size of Cu ZnO and ZrO_2 sepecies and the reduced surface content of Cu species on the reduced catalyst.

Table 4. Catalytic performance of as-prepared catalysts.[a]

Catal.	CO_2 conv. (%)	Selectivity (C-mol %)		
		CH_3OH	CO	Others
CuZnZr(CP)	26.7	55.2	44.6	2.01×10^{-1}
CuZnZr-H_2O	15.6	64.1	34.7	1.20
CuZnZr-TPABr*	11.4	92.7	6.80	4.97×10^{-1}
CuZnZr(CP)[b]	11.3	60.5	39.3	2.04×10^{-1}

[a] Reaction conditions: 5.0 MPa; 250 °C; 3000ml/g/h; 6.0h; $H_2/CO_2/N_2$=69/23/8; * CuZnZr-TPABr = CuZnZr-TPABr-2d; [b] Reaction conditions: 5.0 MPa; 250 °C; 55000ml/g/h; 6.0h; $H_2/CO_2/N_2$=69/23/8.

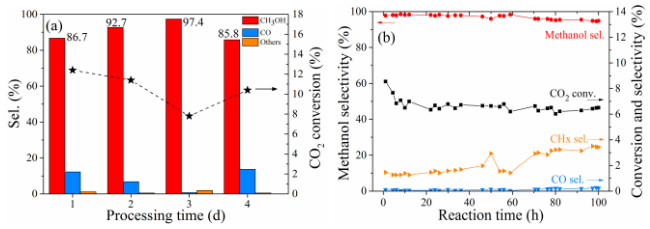

Figure 7. Catalytic performance of (a) the CuZnZr catalysts treated by TPABr with different processing time; (b) the stability test of the CuZnZr-TPABr-3d. Reaction conditions: 5.0 MPa; 250 °C; 3000 ml/(g · h); $H_2/CO_2/N_2$=69/23/8.

The catalysts treated by TPABr with different processing time were also used for CO_2 hydrogenation and the results are shown in Fig. 7(a). It is noted that the processing time has control of the product distribution in our catalytic system. The CH_3OH selectivity increases gradually with the elevation of processing time within 1-3 days, and reaches a maximum of 97.4% on CuZnZr-TPABr-3d catalyst. Further increase of processing time (eg. CuZnZr-TPABr-4d catalyst) leads to an obvious decrease of selectivity. The CO_2 conversion first declines and then increases with increasing processing time. The maximum CH_3OH selectivity of 97.4% and minimum CO_2 conversion of 7.82% are obtained in the 3 day catalyst, indicating the further passivation of the catalyst. The selectivity of by-product CO first declines and then increases with increasing processing time. The CuZnZr-TPABr-3d catalyst shows the minimum selectivity of CO.

Table 5. Distribution of CO_2 conversion of as-prepared catalysts.[a]

Catal.	CO_2 conv. (%)	
	To CH_3OH	To CO
CuZnZr(CP)	14.7	11.9
CuZnZr-H_2O	10.0	5.41
CuZnZr-TPABr*	10.6	7.75×10^{-1}
CuZnZr-TPABr-1d	10.8	1.51
CuZnZr-TPABr-3d	7.62	5.49×10^{-2}
CuZnZr-TPABr-4d	8.92	1.42

[a] Reaction conditions: 5.0 MPa; 250 °C; 3000ml/g/h; 6.0h; $H_2/CO_2/N_2$=69/23/8;
* CuZnZr-TPABr = CuZnZr-TPABr-2d.

Further, from the Table 5 for CO_2 conversion contributing to methanol and CO respectively, it is noted that the effect of VPT process on CO_2 conversion to CO is rather severer than CO_2 conversion to methanol. Especially the conversion of CO_2 to CO decreases dramatically from 11.9% over CuZnZr(CP) to 0.775% over CuZnZr-TPABr, indicating that RWGS reaction is mostly inhabited. Nie et al.[34] mentioned two possible paths for methanol formation from CO_2: the "formate" path (direct hydrogenation), and the "RWGS + CO-hydro" path (with reverse water gas shift step). Our results indicate apparently that the "RWGS + CO-hydro" path is not well running on the catalyst treated using TPABr. It is plausible that the VPT process using TPABr with different processing time can tune the product distribution through restriction of RWGS reaction.

In combination of the catalyst test, the increase in particle size apparently leads to the decrease of CO_2 conversion. However, the CuZnZr-H_2O and CuZnZr-TPABr, which have a similar size of particle, show obviously different catalytic performance, wherein, the latter shows relatively lower CO_2 conversion and higher methanol selectivity. Therefore, it seems that the particle size of Cu is not directly related to methanol selectivity. In combination of the above test of activity, the formation of the rod-like structure might be helpful for high-selectivity methanol production.[23]

According to the CO_2-TPD results above, the VPT method dramatically weakens the adsorption ability of CO_2 on catalyst surface which easily leads to a decrease in amount of CO_2 residue on catalyst surface in present CO_2 hydrogenation. It is deduced that the decrease of CO_2 conversion is resulted from the decrease in amount of CO_2 residue on catalyst. Based on operation temperature of 250 °C, the present CO_2 hydrogenation is closely related to the basic sites ascribed to β and γ in CO_2-TPD profiles. Thus, relatively higher desorption peak area of CuZnZr-H_2O catalyst than that of CuZnZr-TPABr catalyst (Figure 6(c)) is seemingly responsible for slightly higher CO_2 conversion. The strong basic sites on catalyst surface have been reported to be obviously promotional for CO_2 hydrogenation into methanol.[23] Here, we made the functions of CH_3OH selectivity and proportion of strong basic sites with the processing time over the CuZnZr-TPABr-nd catalysts (shown in Fig. S4). It is noted that the plotted curves have similar volcano trends. Therefore, it is drawn a conclusion reasonably that the more proportion of strongly basic sites are favorable for methanol synthesis.

Our above XPS results have revealed that Zn and Zr are enriched on catalyst surface after VPT process using TPABr. The Zn migrated in the active phase is regarded to consist most probably of an oxygen deficient.[36] This VPT process using TPABr facilitates the generation of more oxygen vacancies which are effective for methanol production as the previous literatures[24,37,38] had pointed out. Moreover, the concentration of oxygen vacancies can be tuned through changing the processing time as mentioned above (Table 3). Here, we associated the methanol selectivity with the percentage of $O_β$ peak (surface-adsorbed oxygen which is related to the presence of oxygen vacancies), as shown in Fig. 5(d). The methanol selectivity is proportional to the concentration of $O_β$ peak, indicating that oxygen vacancies are beneficial to improve the methanol selectivity. However, the total oxygen content among the as prepared catalysts seems to be not directly relevant to methanol selectivity or catalytic activity.

According to the Kirkendall effect,[39] a cross migration of Cu and Zn engenders a surface Zn enrichment which correlates to the catalyst activity.[40-42] However, CuZnZr-H_2O catalyst merely shows the enrichment of Zr without the enrichment of Zn on catalyst surface. Comparing the methanol selectivity over CuZnZr-TPABr catalyst (92.7%) and CuZnZr-H_2O catalyst (64.1%), it is found that the simultaneous enrichment of Zn and Zr on CuZnZr catalyst surface is in favor of improving the

methanol selectivity. The degree of surface enrichment of Zn and Zr can be tuned through changing the VPT processing time as mentioned before (Fig. 4(a)). Here, we associated the methanol selectivity with the degree of surface enrichment of Zn and Zr, as shown in Fig. 8. The methanol selectivity is proportional to the degree of surface enrichment of Zn. However, with increasing the enrichment of Zr, the methanol selectivity frist increses and than decreases, indicating that abundant surface enrichment of Zn and proper enrichment of Zr are favorable to improve methanol selectivity.

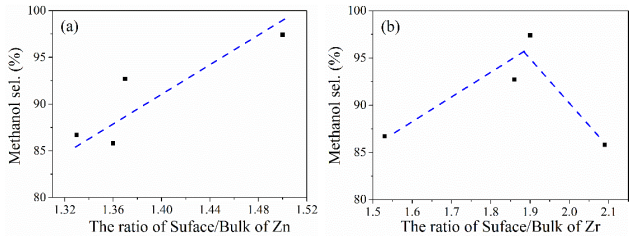

Figure 8. The relationship between methanol selectivity and the ratio of surface/bulk of (a) Zn and (b) Zr.

Furthermore, we considered that the enrichment of Zn and Zr on catalyst surface might cover a part of active site over Cu-based catalyst using for the methanol synthesis and RWGS reaction in varying degrees, leading to a decrease in catalytic activity. However, the binary Zn-Zr is also active for highly-selective CO_2 hydrogenation into methanol in spite of relatively low conversion as reported,[24] which indicates that the enrichment of Zn and Zr on catalyst surface is able to supply amount of new active site for the methanol synthesis. The overall result is that the catalytic ability of RWGS reaction is dramatically restricted, however, the catalytic ability of methanol synthesis is partly retained, resulting that the CuZnZr-TPABr catalyst shows a higher methanol selectivity and relatively lower CO selectivity, just as shown in Table 5. In the meantime, the enrichment of Zn and Zr on the CuZnZr catalyst surface might also obstruct the reduction of surface Cu^{2+} species, which might passivate the activity of Cu species to a certain extent, leading to the decrease in CO_2 conversion. In order to investigate whether the activity of Cu species over the VPT catalysts using TPABr is totally disabled on the reaction of CO_2 hydrogenation to methanol, we compared the catalytic performance of CuZnZr-TPABr-3d catalyst (Cu:Zn:Zr = 6:3:1 mol ratio) and ZnZr catalyst (Zn:Zr = 3:1 mol ratio), as shown in Table S2. Although these two catalysts show similar catalytic activity, the methanol selectivity on them is disparate. The methanol selectivity over CuZnZr-TPABr-3d catalyst is higher than that over ZnZr catalyst, indicating that the Cu species over the VPT catalysts still play a part in the dissociation of hydrogen, where the function of hydrogenation over Cu species is partly weakened.

Optimized experiments show the treatment temperature within 180-200 °C are suitable for highly-selective methanol production (Table S3). In addition, the durability of the CuZnZr-TPABr-3d catalyst for CO_2 hydrogenation to methanol was measured over a 100 h period as shown in Fig. 7(b). It can be found that methanol selectivity is well kept (above 95%) within reaction time and only CO_2 conversion decreases slightly at early stage of 0-4 h reaction. This indicates that our catalyst treated using VPT is significantly potential to the methanol production from CO_2.

There needs to be said, although we attempted to explore whether TPA^+ or Br^- plays a vital role in the treatment to CuZnZr(CP), unfortunately it still retains unclear by now, which needs to be in-detail studied in next work through the designed preparation of catalyst.

Conclusions

Main Text Paragraph. In this paper, we have investigated the effect of vapor-phase-treatment (VPT) to the CuZnZr samples on the suface physicochemical properties and the performance of the resulting catalysts in CO_2 hydrogenation to methanol. Detailed studies were done to clarify the reason that VPT treament leads to the changed reaction behaviors of the catalysts. When using TPABr as the treatment reagent, the rod-like particles with Zn as main body are formed on the CuZnZr-TPABr catalyst and the size of CuO particles dramatically increases. Moreover, this VPT process with TPABr induces the changes on elemental composition containing simutaneous enrichment of Zn and Zr and oxygen species distribution (mainly increasing concentration of oxygen vacancies), and obviouly decreases amounts of weak basic sites. Furthermore, the most obvious change occoures on the catalyst with the porcessing time of 3 day (CuZnZr-TPABr-3d), lying in a high enrichment of Zn, a proper enrichment of Zr and more content of oxygen vacancies. Increased particle size of CuO and proper suface enrichment of Zn and Zr makes the activity of Cu species for CO_2 hydrogenation be crippled dramatically, however the activity of dissociation of hydrogen over Cu species is still remained. These synergetic effects finally lead to an excellent methanol selectivity. The CuZnZr-TPABr-3d catalyst shows the methanol selectivity of 97.4 % and a favorable durability. The experiment with high space velocity demonstrated that VPT with TPABr is favourable for improving selectivity of methanol and but not simply decrease the catalytic activity in CO_2 conversion, despite that a certain degree of passvation occurs. Further mechanistic study and a wider screen of catalysts are underway.

Experimental Section

Preparation of catalysts

CnZnZr(CP) catalyst. The CuZnZr catalyst, a tri-component catalyst consisting of Cu, Zn and Zr (Cu/Zn/Zr = 6:3:1 mol ratio), was prepared by a conventional co-precipitation method. Typically, an aqueous solution of $Cu(NO_3)_2 \cdot 6H_2O$, $Zn(NO_3)_2 \cdot 6H_2O$, and $ZrO(NO_3)_2 \cdot 2H_2O$ (1 M, 500 mL) and a solution of Na_2CO_3 precipitant (1 M, 500 mL) were added dropwise to deionized water (500 mL) simultaneously under stirring at 65 °C. The pH during precipitation was kept at a constant value of 7.0. The resulting suspension was aged for 2 h, then filtered and washed with distilled

water. Finally, the cake was dried at 110 °C for 12 h, followed by calcination in muffle overnight at 350 °C for 4 h. Obtained sample was denoted as CuZnZr(CP) catalyst.

CuZnZr(VPT) catalyst. Vapor-phase-treatment process was operated in an autoclave containing the Teflon liner. In a typical process, the powdered CuZnZr(CP) sample was placed on Teflon liner with a Teflon interlayer, and the aqueous solution of vapor-phase-treatment reagent was added into the bottom of the Teflon liner. In our experiments, the quantity of the treatment reagents is equaled to that of CuZnZr(CP) catalyst. The treatment is operated at 180 °C for 2 days. The obtained sample was dried at 110 °C for 12 h, and then calcined at 550 °C for 4 h. Wherein, the CuZnZr catalysts treated with no any vapor-phase reagent but deionized water was denoted as CuZnZr-H_2O and the CuZnZr catalysts treated by TPABr were denoted as CuZnZr-TPABr, respectively. Otherwise, the CuZnZr(CP) catalyst was also treated with TPABr for 1 ,3 and 4 days respectively, and the obtained catalysts were denoted as CuZnZr-TPABr-1d, CuZnZr-TPABr-3d and CuZnZr-TPABr-4d, wherein, above-mentioned CuZnZr-TPABr catalyst is equivalent to CuZnZr-TPABr-3d catalyst. As comparison and reference, some additional TPABr treated catalysts with different vapor-phase-treatment temperature were prepared in our experiments. Wherein, treatment temperature is 120 °C, 140 °C, 160 °C, 180 °C, 200 °C, respectively. The obtained samples were dried at 110 °C for 12 h, and then calcined at 550 °C for 4 h. Other operation conditions/parameters are similar with that for preparing CuZnZr-TPABr-3d catalyst.

Characterization methods

Powder X-ray diffraction patterns (XRD) were recorded over the 2θ range from 5° to 80° using a Rigaku MiniFlex II X-ray diffractometer, which was operated at 40 kV and 40 mA with Cu Kα radiation (k = 0.15418 nm).

H_2-temperature-programmed reduction (H_2-TPR) was performed to investigate the reducibility of the catalysts using a chemisorption instrument (TP-5080). The catalyst (50 mg) was pretreated at 300 °C under a flow of N_2 (30 ml/min) for 1 h and then cooled to 50 °C; after cooling, the flow was switched to a H_2/N_2= 0.09 mixture (35 ml/min). The temperature-programmed reduction was performed from 100 °C to 600 °C with a heating rate of 10 °C/min.

CO_2 temperature programmed desorption (CO_2-TPD) measurements were carried out on an AMETEK mass spectrometer to monitor the desorption of CO_2. In each experiment, the sample was reduced at 300 °C for 4 h with diluted hydrogen (10% H_2 in N_2). After cooling down to 50 °C, the catalyst was exposed on CO_2 flow for 1 h, and then flushed with Ar until the baseline is stable. The CO_2 desorption was performed from 50 °C to 600 °C with a heating rate of 10 °C/min and the signal was recorded by thermal conductivity detector (TCD).

The specific surface area (SA) of the catalysts was calculated according to the BET method using the N_2 adsorption isotherm obtained on a Micromeritics ASAP 2020 gas adsorption device.

The morphology of the catalysts was investigated with a FET XL30S-FEG scanning electron microscopy (SEM) with an accelerating voltage of 10.0 kV.

TEM, dark-field scanning TEM (STEM) and energy dispersive X-ray spectroscopy (EDS) measurement was carried out on a JEM-2100F high resolution transmission electron microscopy operated at 200.0 kV.

X-ray photoelectron spectroscopy (XPS) measurement was performed on an AXIS ULTRA DLD spectrometer with a monochromatic Al K (1486.8 eV) source. The obtained binding energies were calibrated using the C1s peak (284.6 eV) as the reference. The experimental error is within ±0.1 eV. A beam voltage of 3 kV was supplied to the Ar ion gun with an emission current of 25 mA. During Ar ion sputtering, the pressure of the analysis chamber was maintained at < 10^{-6} Torr. Radiation energy of Ar ion beam is 2 k eV.

The bulk analytical composition of the catalysts was determined by XRF measurements, using a Bruker AXS-S4 Explorer spectrometer, equipped with a Rhodium X-ray source (Rh anode and 75 μm Be-window), a LiF 220 crystal analyzer and a 0.12° divergence collimator. Raman scattering spectroscopy was measured using a diode-pumped solid state laser of wavelength 533 nm with a power of 50mW.

Catalytic evaluation of catalysts

The CO_2 hydrogenation was performed in a fixed bed stainless steel tubular reactor (with 15.5 mm in inner diameter, 500 mm in length). In a typical experiment, the 3 g catalyst was packed in the reactor. The pre-reduction was conducted using a stream of diluted hydrogen (10% H_2 in N_2) at 300 °C for 10 h. After pre-reduction, the reaction was run at temperature 250 °C and pressure 5.0 MPa, using a feed gas ($H_2/CO_2/N_2$=69/23/8) at a space velocity of 3000 mL/g_{cat}/h. The effluent products were kept in gaseous state by electronic heater and analyzed online by a gas chromatograph with thermal conductivity detector (TCD), using carbon molecular sieve column for hydrogen, carbon monoxide and methane. The selectivity of hydrocarbon products was measured online by another gas chromatograph with a hydrogen flame ionization detector (FID), using GDX-403 column for hydrocarbons, methanol and dimethyl ether. N_2 was used as the internal standard for chromatographic analysis. The analytical results from different gas chromatographs were correlated by methane concentration.

Acknowledgements

This work was supported by the Key Science and Technology Program of Shanxi Province, China (MD2014-10), National Natural Science Foundation of China (21573269, 21603258), and Natural Science Foundation of Shanxi Province (201601D202015), China.

Keywords: CO_2 hydrogenation • methanol • vapor-phase-treatment • CuZnZr catalyst

[1] M. Aresta, in: M. Maroto-Valer (Ed.), Carbon Dioxide Capture and Storage, Woodhead Publishing Limited, Abington Hall, Granta Park, Cambridge, CB216AH, UK, 2009.

[2] G. Centi, E.A. Quadrelli, S. Perathoner, *Energy Environ. Sci.* **2013**, 6, 1711-1731.

[3] G. Centi, S. Perathoner, *Catal. Today* **2009**, 148, 191-205.

[4] A. Álvarez, et al, *Chem. Rev.* **2017**, 117, 9804-9838.

[5] G.A. Olah, G.K.S. Prakash and A. Goeppert, *J. Am. Chem. Soc.* **2011**, 133, 12881-12898.

[6] Y.-F. Zhao, Y. Yang, C. Mims, C.H.F. Peden, J. Li, D. Mei, *J. Catal.* **2011**, 281, 199-211.

[7] M.P. Rohde, D. Unruh, G. Schaub, *Ind. Eng. Chem. Res.* **2005**, 44, 9653-9658.

[8] O. Ayodele, *J. CO_2 Util.* **2017**, 20, 368-377.

[9] S. Kattel, P. J. Ramirez, J. G. Chen and Rodriguez, *Science* **2017**, 355, 1296-1299.

[10] R. Van den Berg, et al, *Nat. Commun.* **2016**, 7, 13057.

[11] S. Natesakhawat, J.W. Lekse, J.P. Baltrus, P.R. Ohodnicki Jr., B.H. Howard, X. Deng, C. Matranga, *ACS Catal.* **2012**, 2, 1667-1676.

[12] F. Arena, G. Italiano, K. Barbera, S. Bordiga, G. Bonura, L. Spadaro, F. Frusteri, *Appl. Catal. A: Gen.* **2008**, 350, 16-23.

[13] J. Sloczynski, R. Grabowski, P. Olszewski, A. Kozlowska, J. Stoch, M.Lachowska, J. Skrzypek, *Appl. Catal. A: Gen.* **2006**, 310, 127137.
[14] L. Li, D. Mao, J. Yu, X. Guo, *Journal of Power Sources* **2015** 279, 394-404.
[15] F. Arena, G. Mezzatesta, G. Zafarana, G. Trunfio, F. Frusteri, L. Spadaro, *J. Catal.* **2013**, 300, 141-151.
[16] F. Arena, K. Barbera, G. Italiano, G. Bonura, L. Spadaro, F. Frusteri, *J. Catal.* **2007**, 249, 185-194.
[17] P. Gao, F. Li, H. Zhan, N. Zhao, W. Wei, H. Wang and Y. Sun, *J. Catal.* **2013**, 298, 51-60.
[18] N. J. Brown, J. Weiner, K. Hellgardt, M. S. P. Shaffer and C. K. Williams, *Chem. Commun.* **2013**, 49, 11074-11076.
[19] K. Schutte, H. Meyer, C. Gemel, J. Barthel, R.A. Fischer and C. Janiak, *Nanoscale* **2014**, 6, 3116-3126.
[20] B. An, J. Zhang, K. Cheng and W. Lin, *J. Am. Chem. Soc.* **2017**, 139, 3834-3840.
[21] Z. Liang, P. Gao, Z. Tang, M. Lv, Y. Sun, *J. CO_2 Util.* **2017**, 21, 191-199.
[22] V. Deerattrakul, P. Dittanet, M. Sawangphruk, P. Kongkachuichay, *J. CO_2 Util.* **2016**, 16, 104-113.
[23] X. Dong, F. Li, N. Zhao and Y. Tan, *Appl. Catal. B: Environ.* **2016**, 191, 8-17.
[24] J. Wang, G. Li, Z. Li, C. Tang and C. Li, *Sci. Adv.* **2017**, 3, No. e1701290.
[25] Molly Meng-Jung Li, Ziyan Zeng, Fenglin Liao, Xinlin Hong, Shik Chi Edman Tsang; *J. Catal.* **2016**, 343, 157-167.
[26] Muhammad Zahiruddin Ramli, Syed Shatir A. Syed-Hassan, Abdul Hadi; *Fuel Processing Technology,* **2018**, 169, 191-198.
[27] G. Wang, Y. Zuo, M. Han, J. Wang, *Appl. Catal. A Gen.* **2011**, 394, 281-286.
[28] P. Gao, F. Li, F. Xiao, N. Zhao, N. Sun, W. Wei, L. Zhong, Y. Sun, *Catal. Sci. Technol.* **2012**, 2, 1447-1454.
[29] P. Gao, L. Zhong, L. Zhang, H. Wang, N. Zhao, W. Wei, Y. Sun, *Catal. Sci. Technol.* **2015**, 5, 4365-4377.
[30] C. Zhang, C. Wang, W. Zhan, Y. Guo, G. Lu, A. Baylet and A. Giroir-Fendler, *Appl. Catal. B: Environ.* **2013**, 129, 509-516.
[31] L. B. Hoch, et al, *Adv. Sci.* **2014**, 1, 1400013.
[32] G. Bonura, M. Cordaro, C. Cannilla, F. Arena and F. Frusteri, *Appl. Catal. B: Environ.* **2014**, 152, 152-161.
[33] Y. Zhao, Y. Yang, C. Mims, J. Li and D. Mei, *J. Catal.* **2011**, 281, 199-211.
[34] F. Arena, G. Italiano, K. Barbera, G. Bonura, L. Spadaro, F. Frusteri, *Catal. Today* **2009**, 143, 80-85.
[35] X. Nie, X. Jiang, X. Guo and C. Song, *ACS Catal.* **2018**, 8, 4873-4892.
[36] C. Tisseraud, C. Comminges, A. Habrioux, S. Pronier, Y. Pouilloux, *Molecular Catalysis,* **2018**, 446, 98-105.
[37] J. Ye, C. Liu, D. Mei and Q. Ge, *ACS Catal.* **2013**, 3, 1296-1306.
[38] P. Gao, S. Li, X. Bu, S. Dang, Z. Liu, H. Wang, L. Zhong, M. Qiu, C. Yang, W. Wei and Y. Sun, *Nat. Chem.* **2017**, 9, 1019-1024.
[39] C. Tisseraud, T. Comminges, H. Belin, A. Ahouari, Y. Soualah, A. Pouilloux, *J. Catal.* **2015**, 330, 533-544.
[40] S. Kuld, C. Conradsen, P.G. Moses, I. Chorkendorff, J. Sehested, *Angew. Chem. Int. Ed.* **2014**, 53, 5941-5945.
[41] C. Holse, C.F. Elkjær, A. Nierhoff, J. Sehested, I. Chorkendorff, S. Helveg, J.H.Nielsen, *J. Phys. Chem. C* **2015**, 119, 2804-2812.
[42] C. Tisseraud, C. Comminges, Y. Pronier, A. Pouilloux, *J. Catal.* **2016**, 343, 106-114.

Entry for the Table of Contents (Please choose one layout)

FULL PAPER

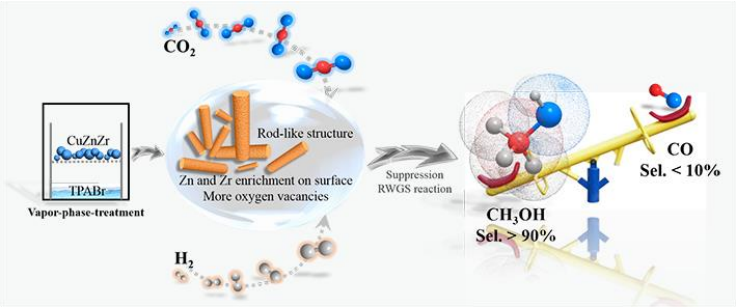

Shuyao Chen, Junfeng Zhang, Peng Wang, Xiaoxing Wang, Faen Song, Yunxing Bai, Meng Zhang, Yingquan Wu, Hongjuan Xie and Yisheng Tan**

Page No. – Page No.

Effect of vapor-phase-treatment to CuZnZr catalyst on the reaction behaviors in CO_2 hydrogenation into methanol

VPT with TPABr promoted the formation of the rod-like structure, Zn and Zr enrichment on surface and the presence of more concentration of oxygen vacancies on CuZnZr catalyst, suppressing RWGS reaction. CuZnZr-TPABr catalyst shows a methanol selectivity above 90%.